OPTIMIZATION OF THE C/SiC THRUST CHAMBER FOR A 400N THRUSTER

Georg Fleischmann, Ernst Dieter Sach

Daimler-Benz Aerospace AG
Space Infrastructure
Munich, Germany

ABSTRACT

In order to minimize the stresses in the laminate, an optimization analysis was performed with MSC/NASTRAN. Design variables were ply thicknesses and fiber orientations. The results showed that the stresses perpendicular to the fibers cannot be influenced because they are primarily caused by the temperatures loads. The shear stresses, however, could be reduced by a factor of 2 compared with a quasi-isotropic lay-up.

1. Description of Thrust Chamber

Propulsion systems with a thrust of 400N are primarily applied to inject a satellite from the geostationary transfer orbit reached by the launch vehicle into the 24 hour orbit. The fuel is monomethyl hydrazine with nitrogen tetroxide as oxydator.

The thrust chambers used up to now for the 400N thrusters are made from stainless steel. Because of the high temperature especially in the nozzle throat the thrust chamber will be generatively cooled. In order to avoid the cooling effort, materials resistant to high temperature and oxidation like platinum/rhodium and fiber reinforced ceramics are of increasing interest. Due to the much lower density of fiber ceramics a considerable weight reduction is additionally achieved in this case. Fig. 1 shows such a thrust chamber in C/SiC, where the fibers consist of carbon and the matrix is made from silicon carbide. The dimensions can be seen in Fig. 2.

Figure 1: C/SiC Thrust Chamber

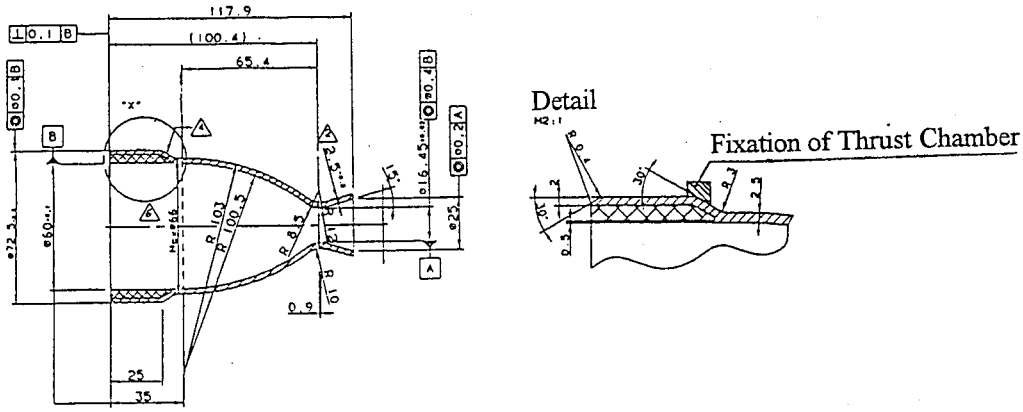

Figure 2: Dimensions of the C/SiC Thrust Chamber

2. Material Properties

The typical material properties of a unidirectional C/SiC composite are shown in fig. 3. Characteristic for all fiber reinforced materials are the high strength and stiffness values in fiber direction and relatively low values perpendicular to the fibers and for shear. Please note the different thermal expansion coefficients parallel and normal to fiber direction.

Tensile Strength	$\sigma_{\parallel z}$	MPa	470
Compression Strength	$\sigma_{\parallel d}$	MPa	1000
Tensile Strength	$\sigma_{\perp z}$	MPa	50
In-plane Shear Strength	$\tau_{\parallel\perp}$	MPa	10
Modulus of Elasticity	$E_{\parallel}$	GPa	150
Modulus of Elasticity	$E_{\perp}$	GPa	14
Shear Modulus	$G_{\parallel\perp}$	GPa	10
Poisson's Ratio	$\nu_{\parallel\perp}$		0.1
Thermal Expansion Coefficient	$\alpha_{\parallel}$	1/K	$1.6 \cdot 10^{-6}$
Thermal Expansion Coefficient	$\alpha_{\perp}$	1/K	$6.3 \cdot 10^{-6}$
Density	ρ	g/cm³	2.0

Figure 3: Material Properties of a Unidirectional C/SiC Composite

3. Loads

The design of the C/SiC thrust chamber is based on the following loads:

a) Cooling of the chamber from processing temperature t_1 = 1600 C down to t_2 = 20 C

b) Bending moment on the chamber caused by 20 g lateral acceleration of the entire propulsion unit (20 g × safety factor of j = 1.5); the resulting maximum force per unit length is 14 N/mm.

c) Pressure in thrust chamber p_i = 15 bar = 1.5 MPa (operating pressure p = 1 MPa × safety factor of j = 1.5).

d) Temperature during operation at a flow rate of M = 133.66 g/s (temperature distribution s. fig. 4).

The temperature loads are regarded to be stationary. The thrust chamber is assumed to be free of stresses at processing temperature of t_1 = 1600 C. By superposition of the loads above, the following load cases were defined:

- load case 1: load a (stress state after manufacturing)
- load case 2: load a + b (flight case launch vehicle)
- load case 3: load a +c (condition at start of propulsion unit)
- load case 4: load a + d (stationary operation)

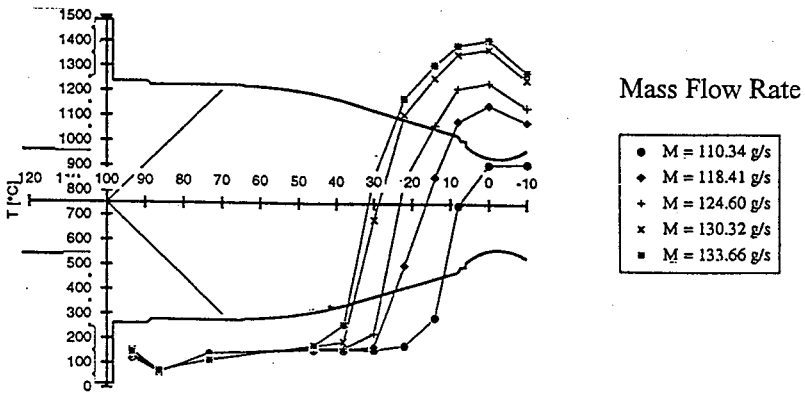

Figure 4: Temperature Distribution in Thrust Chamber

4. Finite Element Model

The decisive investigations were performed with a finite element model representing a small sector of the thrust chamber (s. fig. 5). By applying rotationally symmetric boundary conditions an annular structure is simulated.

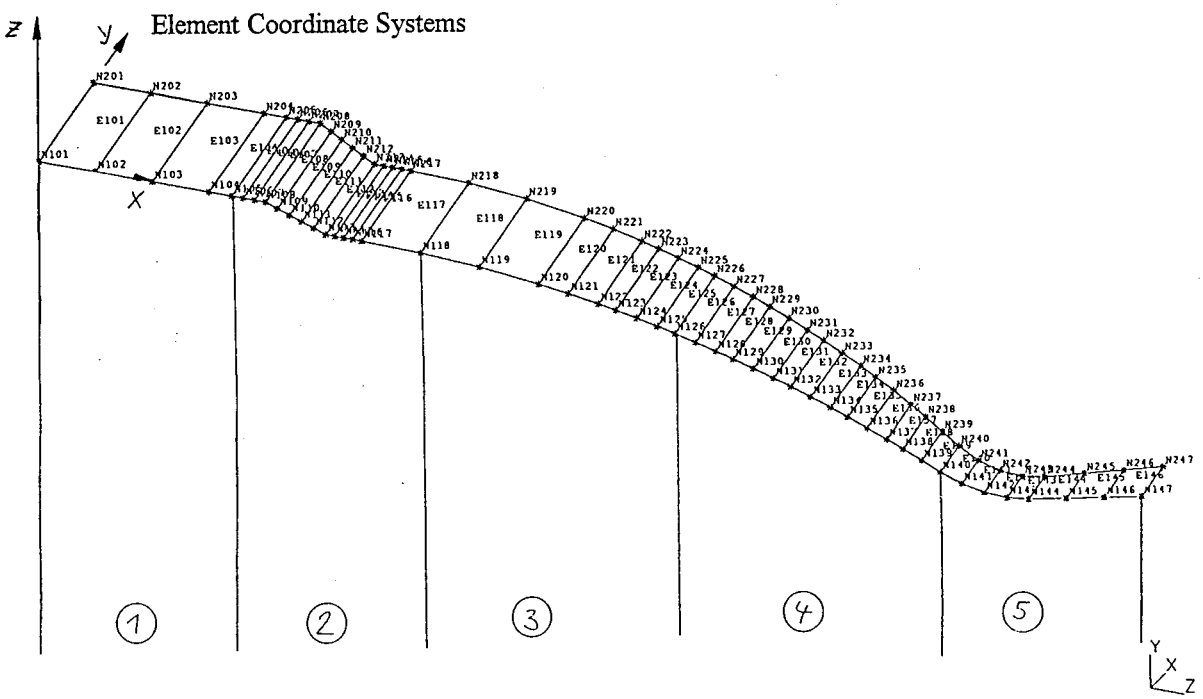

Figure 5: Finite Element Model of the Thrust Chamber

5. Results

5.1 Quasi-Isotropic Laminate

With a quasi-isotropic symmetric laminate consisting of equal numbers of 0°, 90° and ± 45° plies, the resulting maximum stresses are as follows (s. fig. 6):

Load Case	$\sigma_{\parallel}$ N/mm²	$\sigma_{\perp}$ N/mm²	$\tau_{\parallel\perp}$ N/mm²
1	-156	98	7.7
2	-212	100	7.9
3	-184	106	14.4
4	-172	98	13.6
Allowable Value	470 (Tension) 1000 (Compression)	50	10

Figure 6: Maximum Stresses in the Quasi-Isotropic Laminate

It can be identified that the stresses normal to the fibers and the in-plane shear are considerably above the allowables. Fig. 7 shows the highest loaded ply of each element. It can be seen that high stresses occur both at the fixation line of the thrust chamber and in the throat.

5.2 Optimization

In order to minimize stresses an optimization was performed with MSC/NASTRAN, Solution 200. The structure was subdivided into 5 typical sections (s. fig. 5). Design variables were ply thickness and fiber angle. The optimization was started with 12 plies for each section, each ply had a thickness of 1.0 mm. 6 angle positions were defined, 2 of which differ only in the sign. A symmetric stack was assumed. Objective function was the mass, constraints were the allowable stresses.

The first computations showed that with the stress limits given in fig. 3 an optimum could not be found. Only by increasing $\sigma_{\perp}$ to more than 100 N/mm² the computer runs converged. The reason for this high stress normal to the fibers is to be seen in the difference between longitudinal and lateral thermal expansion coefficient of the unidirectional ply and the externally high temperature difference between processing and room temperature.

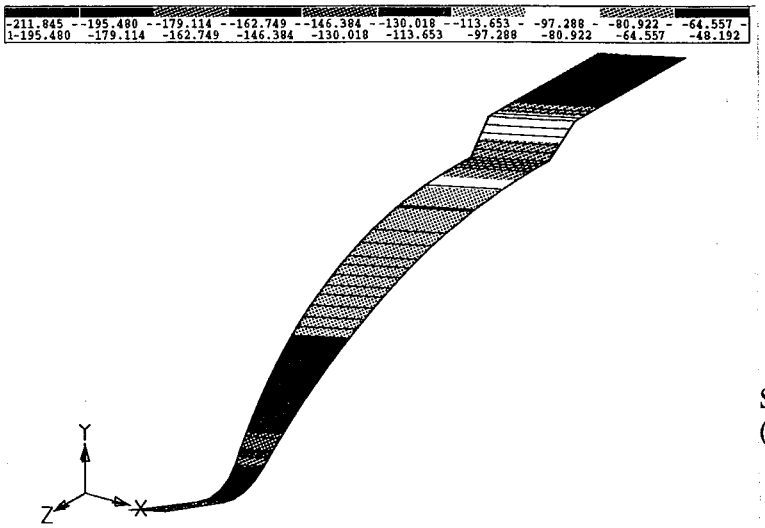

Stresses parallel to fibers
(load case 2)

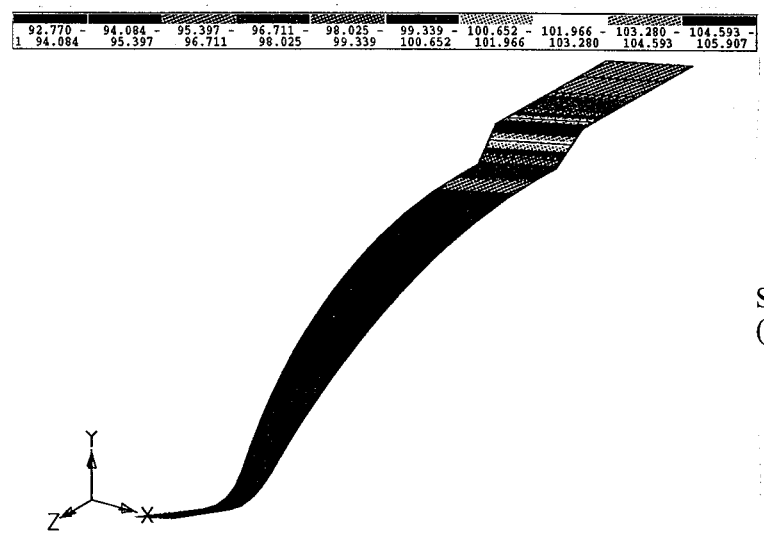

Stresses normal to fibers
(load case 3)

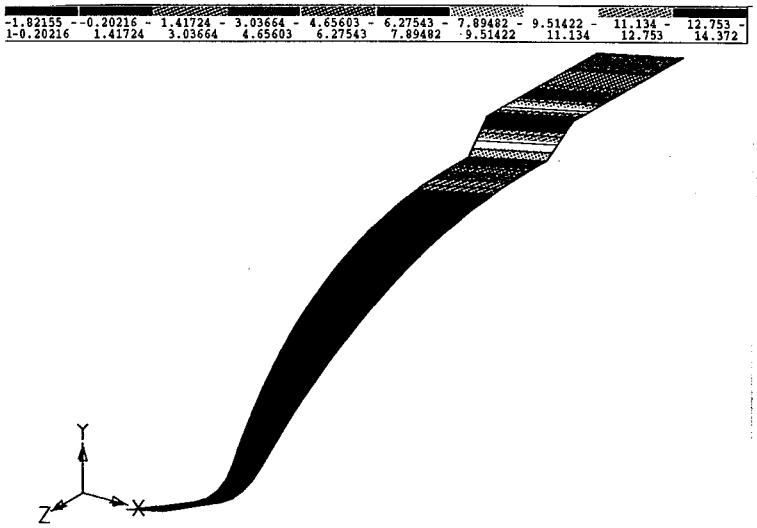

In-plane shear
(load case 3)

Figure 7: Stress Distribution for the Symmetric Quasi-Isotropic Laminate (Ply with Maximum Stress)

Section	Angle	Ply Thickness (4 Layers) mm	Total Thickness of Laminate mm
1	± 82° ± 47° 0°	0.097 0.032 0.18	1.24
2	± 81° ± 30° ± 8°	0.33 0.091 0.64	4.24
3	± 75° ± 44° ± 9°	0.065 0.062 0.093	0.88
4	± 78° ± 49° 0°	0.04 0.05 0.14	0.92
5	± 81° ± 41° 0°	0.2 0.16 0.3	2.64

Figure 8: Result of Optimization

Fig. 8 shows the final result of the optimization. For most of the thrust chamber a wall thickness smaller than 1 mm is sufficient. Larger wall thicknesses are necessary at the fixation of the chamber (about 4.3 mm) and in the throat (about 2.7 mm). The resulting ply angles lie for all section at 0° (fibers longitudinal) and close to 90° (fibers circumferential) and 45°. Only at the fixation a 30° ply is preferable against the 45° ply.

60 % of the thickness belongs to the plies with fibers in longitudinal direction. However, in the throat and in section 3 the content is only 45 %. The percentage of circumferential plies amounts to 30 % for all sectors.

5.3 Proposed Ply Stack

Based on the optimization computation the proposed ply stack is shown in fig. 9. In order to facilitate manufacture an exact adaptation of the wall thickness to the calculation results is not appropriate. Therefore the wall thickness necessary at the fixation area is maintained through the entire cylindrical part of the thrust chamber and the required thickness for the throat is extended to the sections 3 and 4. Due to manufacturing reasons the wall thickness in the narrowest cross section has to be 1.5 times greater than in the vicinity.

The maximum stresses computed for this ply stack are shown in fig. 10. The stress distribution in the thrust chamber is presented in fig. 11.

Evaluating the results it can be recognized that the optimization does not have any essential influence on the stresses in fiber direction and normal to it. These stresses are primarily caused by the temperature difference between processing (stress free state) and room and operating temperature respectively. Variations of the ply stack hardly influence these stresses and therefore an optimization computation cannot achieve an improvement.

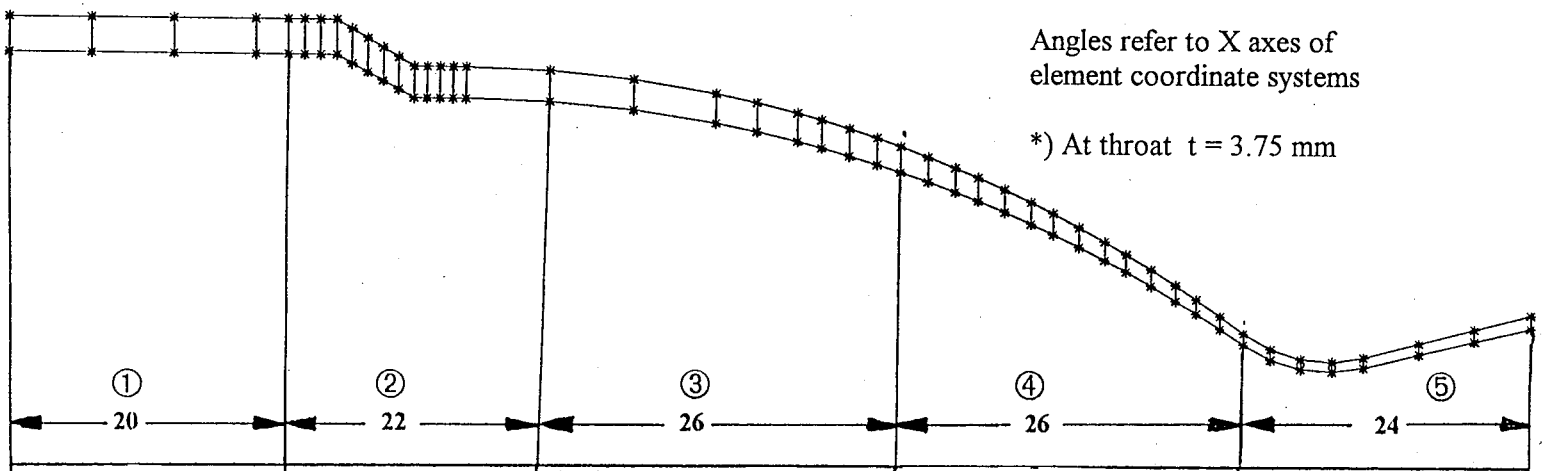

Angle	Thickness	Angle	Thickness	Angle	Thickness	Angle	Thickness	Angle	Thickness
∓ 81°	0,2 0,2	∓ 81°	0,2 0,2	∓ 75°	0,2 0,2	∓ 78°	0,2 0,2	∓ 80°	0,3 0,3
∓ 81°	0,2 0,2	∓ 81°	0,2 0,2	—	—	—	—	—	—
∓ 0°	0,3 0,3	∓ 8°	0,3 0,3	∓ 8°	0,3 0,3	∓ 0°	0,3 0,3	∓ 0°	0,3 0,3
∓ 0°	0,3 0,3	∓ 8°	0,3 0,3	—	—	—	—	—	—
∓ 45°	0,125 0,125	∓ 30°	0,125 0,125	∓ 45°	0,125 0,125	∓ 45°	0,125 0,125	∓ 50°	0,125 0,125
± 45°	0,125 0,125	± 30°	0,125 0,125	± 45°	0,125 0,125	± 45°	0,125 0,125	± 50°	0,125 0,125
± 0°	0,3 0,3	± 8°	0,3 0,3	—	—	—	—	—	—
± 0°	0,3 0,3	± 8°	0,3 0,3	± 8°	0,3 0,3	± 0°	0,3 0,3	± 0°	0,3 0,3
± 81°	0,2 0,2	± 81°	0,2 0,2	—	—	—	—	—	—
± 81°	0,2 0,2	± 81°	0,2 0,2	± 75°	0,2 0,2	± 78°	0,2 0,2	± 80°	0,3 0,3
t = 4,5 mm		t = 4,5 mm		t = 2,5 mm		t = 2,5 mm		*) t = 2,5 mm	

Figure 9: Proposed Ply Stack

Load Case	$\sigma_{\parallel}$ N/mm²	$\sigma_{\perp}$ N/mm²	$\tau_{\parallel\perp}$ N/mm²
1	-142	97	5.8
2	-248	98	5.2
3	-174	104	7.7
4	-163	96	7.3

Figure 10: Maximum Stresses for Optimized Ply Stack

The very high in-plane shear stresses, however, occurring at the fixation of the thrust chamber could be reduced by a factor of 2. By a better adaptation of the wall thickness to the optimization results, a considerable mass reduction can be additionally achieved.

6. Conclusion

With the Solution 200 of MSC/NASTRAN both ply thickness and fiber angle of a laminate can be optimized. For temperature loads a sufficiently high strength normal to the fibers is necessary since the occurring stresses in this direction cannot be influenced in parts with rotational symmetry. In case of the thrust chamber in C/SiC it is presumed that these stresses are reduced by microcracks in the matrix material without causing a failure of the part. Tests planned for the near future will prove this hypothesis.

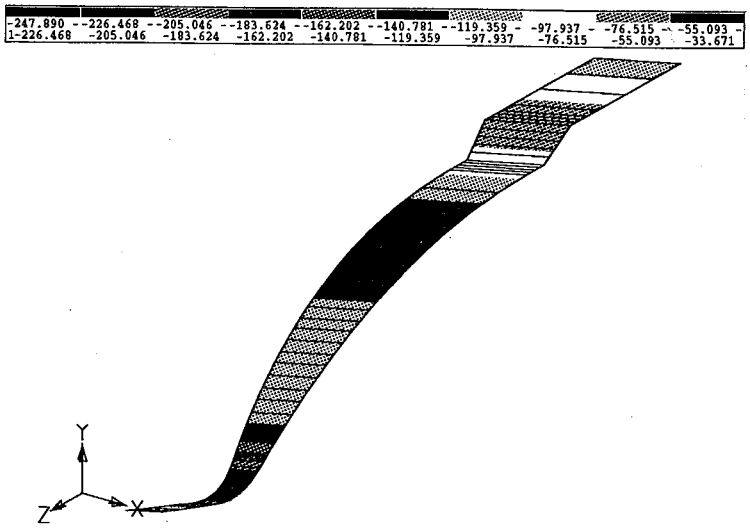

Stresses parallel to fibers
(load case 2)

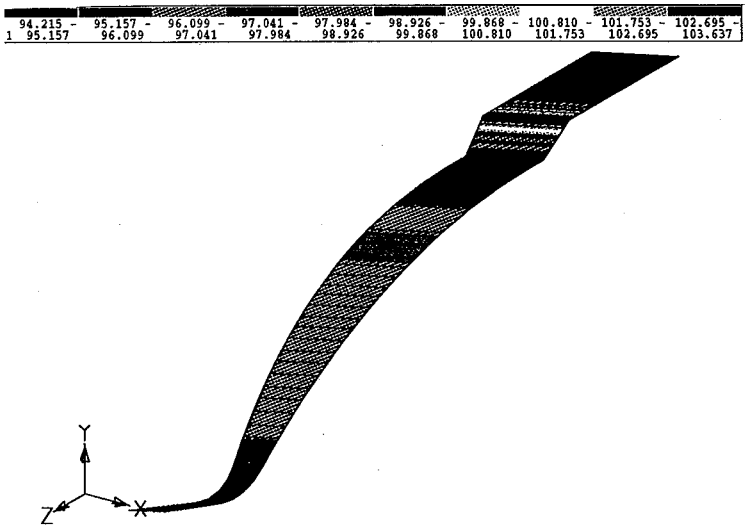

Stresses normal to fibers
(load case 3)

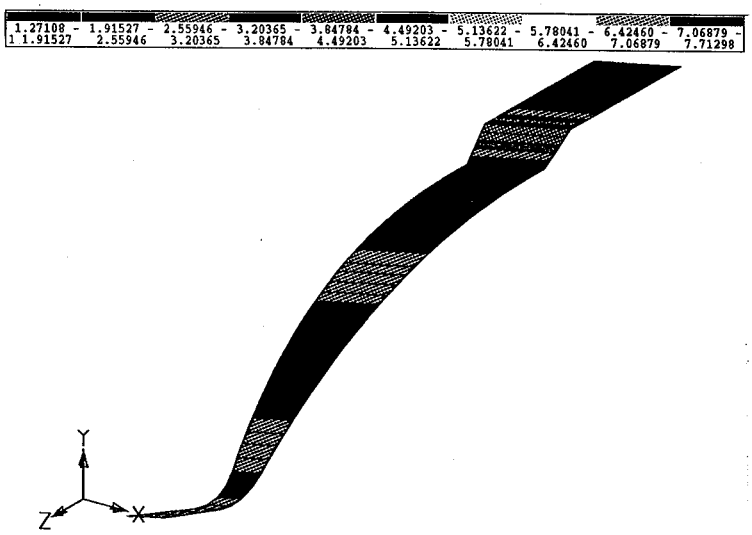

In-plane shear
(load case 3)

Figure 10: Stress Distribution in the Optimized Laminate (Ply with Maximum Stress)